University of Toronto

Physics 479: Final Report

Applications of Control Theory to an Ultracold Atoms Experiment

Digital Feedback Systems for Optical Traps

Author:
Andrew Hardy

Professor:
Dr. Aephraim Steinberg

Abstract

This report will detail the creation and testing of a digital feedback circuit for laser power in the context of a Bose Einstein Condensate project. I will begin with an analysis of the current analog feedback systems in place for the system. From this position, I will motivate the need for upgraded digital feedback loops. In particular, I will focus on the delta-kick cooling [10] [4] laser and its unique requirements suited to a digital feedback system. The bulk of the report will then illustrate the progress made towards realizing a digital feedback system for delta kick cooling or other applications.

1 Introduction

Bose-Einstein Condensation was theorized in 1925 by Albert Einstein [7] after correspondence with Satyendra Nath Bose [6] the year prior which led to the creation of Bose-Einstein statistics. These statistics determine the behavior of particles with integer spin, dubbed bosons. Einstein derived from the probability of states the average number of atoms in a cell, a formula still taught in statistical mechanics courses today. As a consequence of this theory, the fugacity bounds the number of excited particles. This forces the majority of particles into the ground state, forming a condensate.

In 1995, a team of scientists at JILA led by Eric Cornell and Carl Wieman realized a Bose Einstein Condensate (BEC) using Rubidium atoms and a magneto-optical trap (MOT) [5] . Their usage of the theory of laser cooling and trapping (LCT) generated a whole field of precision physics on its own. LCT allows for not just the slowing, or cooling, of atoms, but sophisticated manipulations. This allows for two exciting regimes of study in regards to LCT. First is the powerful applications to our understanding of the world. The second, equally as important, is the precision required in such approaches in order to obtain significant results. Over two decades later, BEC and LCT serve as tools for our group at University of Toronto to probe even more fundamental questions of quantum mechanics.

I will provide a broad overview of some of the optical set-up required to achieve these results.

2 Current Set-Up and Motivation

The BEC group at the University of Toronto aims to measure one of the most fundamental and peculiar quantum effects, quantum tunneling. [9] This time is measured using the Larmor clock approach. This Larmor time measures the dwell time of a particle inside the barrier. This time can best be explained using the language of weak-measurements, but the technical details are beyond the scope of this report.

Instead I will focus on the equally technically process of LCT. Through the specific applications present in our experiment, I hope to motivate the work detailed in the remainder of the report.
A proper discussion on laser cooling begins with a discussion on what the atomic optical concept of temperature refers to. This contrasts a statistical mechanical perspective, where temperature describes a parameter of the state of a closed system in thermal equilibrium with its surroundings. In laser cooling, atoms absorb and scatter light, making considerable changes to the environment. Despite such a system not being in thermal equilibrium, the moniker of "temperature" remains a useful concept. We shall define it as $\frac{1}{2}k_BT = \langle E_k \rangle$, in terms of the Boltzmann's constant, and the average kinetic energy. [8]
The crux of LCT is that lasers, detuned to the Doppler shifts of moving atoms, can collide with photons. Their absorption slows atoms down. There are also a variety of optical techniques, post MOT, to cool atoms to sub-Doppler regimes. The most important use of this cooling, or slowing, of atoms in BEC applications is the compression of phase space density. This requires us to develop a new formalism relying on density matrices, optical Bloch equations, and Liouville's equation in order to discuss non-unitary processes or the optical forces used here, when the forces depend not only on position, but also on velocity. In this context, I will begin the discussion of traps present in the current BEC experiment.

2.1 Optical Traps and Evaporative Cooling

Post-MOT, The current wave-guide for Rb atoms operates at $1064nm$ and serves an Optical Dipole Trap (ODT). The classical macroscopic equivalent are optical tweezers, for which the 2019 Nobel Prize for Physics was awarded.

The trap consists of a strongly focused Gaussian laser beam. The intensity varies across the transverse from the focus following $I(r) = I_0 e^{-r^2/w_0^2}$. [8] This laser is tuned below the resonance. Therefore the ground-state light shift is everywhere negative, maximizing at the centre of the Gaussian beam. Ground state atoms experience an attractive force towards the centre. This force is given by the gradient of the light shift. This is expressed as

$$\boldsymbol{F} \simeq -\frac{\hbar\gamma^2}{8\delta I_s}\nabla I(r)$$

where δ is the detuning and γ is the natural width. Therefore, by computing the gradient, we receive the expression.

$$\boldsymbol{F} \simeq \frac{\hbar\gamma^2}{4\delta}\frac{I_0}{I_s}\frac{r}{w_0^2}e^{-r^2/w_0^2}$$

In addition, tuning of the laser parameters allow for longitudinal and therefore 3D atomic trapping. This tuning consists of a sufficiently large detuning which decreases the radiation pressure faster than the dipole force. The radiation pressure of the laser beam scales $\frac{1}{\delta^2}$ compared to the dipole force scaling with $\frac{1}{\delta}$. Atoms therefore spend only a small time in the excited / repelled state and are effectively trapped.

2.1.1 Evaporative Cooling

The trap configuration is complicated by a process called evaporative cooling. The potential 'depth' of the optical trap is lowered by decreasing the intensity. Highly energized, 'hot' , atoms evaporate and leave the system. As evidenced by these equations, both frequency and intensity (power density) require precise values and accurate feedback. In particular evaporative cooling requires precise power control to tune the potential height.

2.1.2 Current Analog Feedback

The current power feedback set-up solves most of these requirements. The system takes diverted laser optical power from an Acousto-optic modulator (AOM) This is fed into a photodiode. This current is passed through a resistor and the voltage across this resistor is read by a analog PI box. This box has a notable disadvantage that the gain of the Proportional and Integral components are coupled, limiting the tun-ability of the circuit. The PI box

outputs a voltage between 0 and 1 V into an AOM driver. The optical power has a nonlinear response to the AOM RF power, but through empirical testing based on the response to the atomic cloud, the system works.

2.2 Delta Kick Cooling

Delta-Kick Cooling (DKC), otherwise known as Matter-wave lensing, serves to lower the effective temperature of atoms by collimating the atomic cloud. [10] [4] The process can be described using a Hamiltonian $H_0 = p^2/2m + U(x)$. By extinguishing the potential and subsequently pulsing it, provides a new Hamiltonian,

$$H_k = \frac{p^2}{2m} + V(x)\delta(t - T)$$

. The new potential, defined with a Gaussian time pulse, $\exp\left[-(t-T)^2/2\tau_p^2\right]$, defines the new potential as $\sqrt{2\pi}\tau_p U(x)$ where τ_p is the temporal pulse width. As we extinguish $U(x)$, the atoms gain a spatial spread based on momentum differences. Given sufficient time(T), the momentum of atoms will effectively a linear function of position, $p = m\frac{x}{T}$. By establishing the pulse width based on the free expansion time of the atoms absent of potential, Each kick will reduce the momentum of every atom near zero, given the condition in terms of the frequency of the harmonic potential,

$$\kappa_{\text{cl}} = \sqrt{2\pi}\tau_p\omega^2 T \approx 1$$

This classical description does not give a complete picture of the process, but is sufficient to serve as motivation. As a brief aside, the quantum mechanical picture serves to broaden the position wave function $\psi(x)$, but narrow the width of the the momentum $\phi(p)$ by a factor Q and lower the energy, and effective temperature, by Q^2. This process serves as the temporal matter-wave analog to an optical lens [10]. From this rough treatment, the need for precise power control on the DKC beam becomes apparent. Our DKC procedure consists of two kicks, the first for 1ms, and the second, 15ms later, with half the power. In these narrow time scales, high bandwidth (on the order of $100KHz$)of a feedback system would be critical for accurate and consistent power control. This is currently not feasible from the analog feedback systems described above. A new digital feedback system, however, would allow for control of the DKC beam.

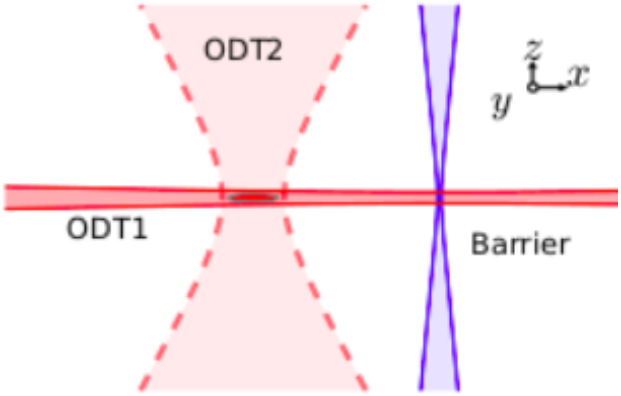

Figure 1: A Diagram from one of the BEC publications detailing the three beams described in this section. ODT1 serves as the wave-guide. ODT2 serves as the DKC beam, and the optical barrier beam is also shown.

2.3 Optical Barriers

Another unique advantage of digital feedback systems is their variable bandwidth. Rather than hardwiring in components to vary the bandwidth, it can be determined by the delay function programmed into Arduino. Our system has unique requirements for accurate bandwidth that may lie within a specific domain. One example of these 'Goldilocks' regimes is feedback on the optical barrier vital to the tunneling experiment.
This beam is $405nm$ laser where the indigo light is detuned to $420nm$, matching the ${}^5S \rightarrow^6 P$ transition of Rb. The barrier height of this light due to the AC stark shift experienced by the atoms is directly proportional to the intensity of the beam. In order to keep a consistent barrier height, the beam is shook at a high enough frequency to appear solid to atoms. Because of these frequency, we require a bandwidth of the feedback system to be quicker than the atoms response to power fluctuations, but slower than the frequency of the beam shakes. In the future, a digital feedback system would also prove to allow us to meet this range more effectively.

3 Present Progress

The current digital feedback circuit (DFC) consists of three components. It begins with an analog to digital conversion (ADC) pin on the chipKIT uC32 micro-controller. This device reads a digital representation of the voltage taken across a resistor connected to the photo-diode. The device then computes a digital correction value using digital PID software. This correction value is converted into binary and fed across the Serial Port Interface (SPI) channels into the digital to analog convertor, an Analog Devices 5780 Evaluation Board. Based on the configuration of that SPI and the DAC itself, it will output a voltage. The following sections will describe in detail the mechanisms of these three components.

3.1 Analog to Digital Conversion

For all experimental concerns, the ADC on the uC32 serves as a black box. However it also serves as the main limiting factor on the bandwidth of the whole DFC, so it warrants adequate explanation. On the uC32, Pins numbered $14-25$ or A0-A11 serve as possible analog inputs. They are in the J7, or ANALOG section of the board. Together with the GND pin, located in J2 or POWER section of the board, analog input is quite simple. [2]
The Arduino Library allows analog input via calling of two functions to specify the pin setting and read out an integer value.

```
pinMode(A0, INPUT);
analogVal = analogRead(A0);
```

This integer value reads with 10 bit precision the voltage value between $0-3.3$ V. The conversion therefore follows the formula

$$V_a = \frac{3.3V_d}{1023}$$

which gives the analog voltage reading in terms of the integer output.
The mechanics of the ADC operate on the principles of successive approximation. [3] This operates through a comparator comparing voltage inputs to voltages coming from a small DAC present in the chip in order to receive an accurate value of the true voltage. On the uC32, the PIC32 processor operates ADC as follows. The analog input is fed through two multi-plexers (MUXs) to one Sample and Hold circuit (SHA). This allows the MUXs to

switch between different analog input pins. The SHA then sends the voltage through a Successive Approximation Register (SAR) through which the actual conversion occurs.

3.1.1 ADC Speed

The conversion is supposed to take 12 clock cycles. One clock cycle for each bit of resolution of the voltage and two clock cycles to complete the conversion. The uC32 operates at 80Mhz, so we should expect approximately 6.6 Mhz conversion rate. The datasheet boats 1Mbsps though. If this means that the pins only sample at 1Mhz, then the conversion rate is only 83 Khz. Experimental testing confirms that the rate is within this order of magnitude.

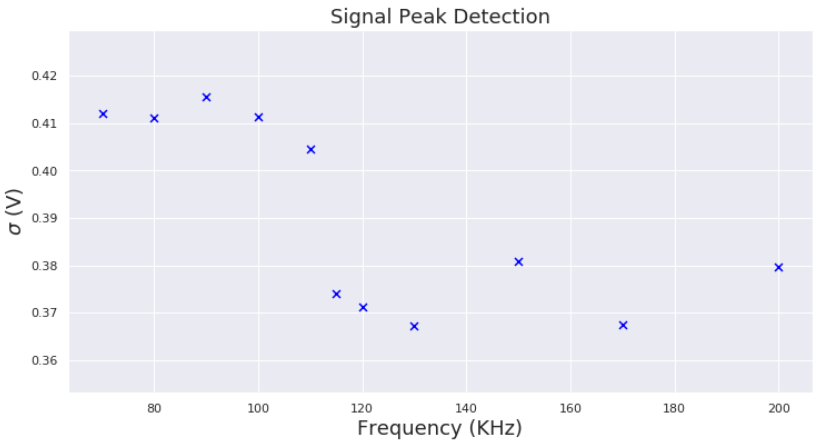

Figure 2: Peak Identification of Sine Wave: Here the standard deviation σ of a sin wave is compared to the frequency of the sin wave. σ serves as roughly the peak of a sine wave. While the signal was set to 0.4V on the Function Generator, due to sampling times, this was incorrectly read above the 100KHz regime.

3.2 PID Controller

The beginning of any study of control theory begins with PID. For the past century, it remains one of the most robust methods to stabilization and control. The basics of PID are the three parameters used in error correction.

Given the formula

$$u(t) = K_{\mathrm{p}} e(t) + K_{\mathrm{i}} \int_0^t e\left(t'\right) dt' + K_{\mathrm{d}} \frac{de(t)}{dt}$$

they are K_i, K_p, K_d, standing for the Proportional, Integral and Derivative. All three of these components serve critical roles in accurate control. I will give brief explanations of the uses of all three of the parameters in the context of laser power control. Then I will give an overview of how to tune the parameters and some progress made in PID simulations in order to best understand the PID.

3.2.1 Parameters and the Ziegler-Nichols Method

The first, and most significant parameter is the proportional gain. This is a simple weight on the error given, $e(t) = S - i(t)$, the difference between the setpoint value and the input signal with noise. If a device had infinite bandwidth, this instantaneous (or instantaneous compared to the speed of noise and drift) correction would wash out the noise and a P controller would be sufficient. Instead, most P control only allows the signal to oscillate around the set point. Every correction misses the mark because of the delay between the read signal and the correction output. In order to remedy this oscillation, the Integral gain allows for a discrete integral accumulation of error measurements. This allows the PID to make cumulative measurements and correct drift in the error signal. This parameter therefore serves to damp the oscillations.

PI controllers serve a large majority of the control community adequately. However, when the error source becomes much more variable, adequate control requires an additional parameter. This is the Derivative gain. Rather intuitively, this gain gives some predictive ability of the error. Derivative gain allows the PID to correct for error that will appear in the signal by the time that the PID outputs a correction. Because of these time sensitivity concerns, it is worth noting that the sampling rate of the integral and derivative components serve to be just as essential. In order to tune these parameters, one of the most robust heuristic methods is dubbed Ziegler -Nichols [11]. It consists of fixing the K_p gain until their are steady oscillations, and then tweaking K_i and K_d in order to damp these oscillations. The Ziegler-Nichols method prescribes specific values based on the response of the system.

3.2.2 Results of PID Simulation

In order to understanding the workings of a PID, I explored the Arduino PID library using simulations. The equation used in the simulation was

$$x_i - x_{i+1} + \frac{1}{5}\sin(10t) + g\omega + n$$

which includes a sinusoidal noise term, a random noise , $n = \pm 1$, and the output w multiplied by some gain factor $g = 1/40$. These values are coded in terms of pure values, not yet converted into voltages.
The behavior of the system follows the expected results of Ziegler Nichols. Once an appropriate gain for the total output was established, relatively naive K_i, K_d parameters were able to control the system. Then through tweaking, a more gentle control system was established.

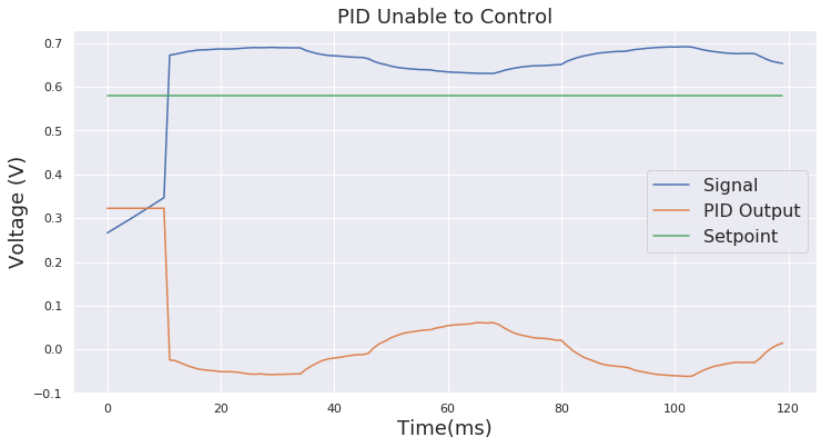

Figure 3: Feedback System with Naive Parameters. The parameters were set to $K_p = 2, K_i = 0, K_d = 0$. This was unable to reach the setpoint.

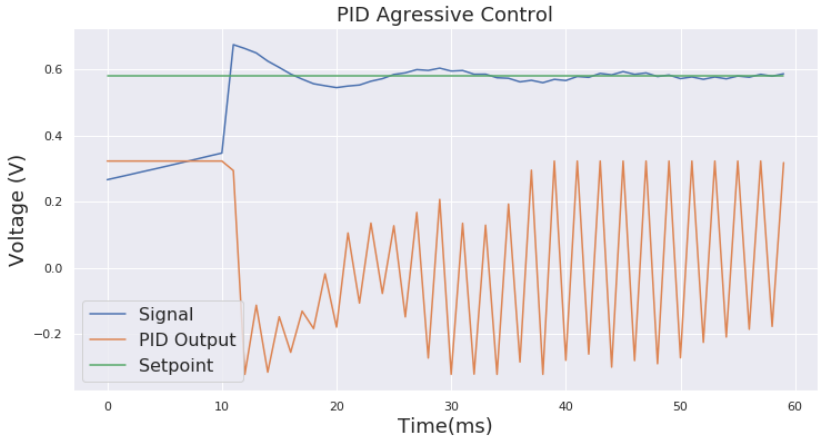

Figure 4: Feedback System with Naive Parameters. The parameters were set to $K_p = 2, K_i = 4.5, K_d = 4$. Notice the extreme oscillations of the PID output.

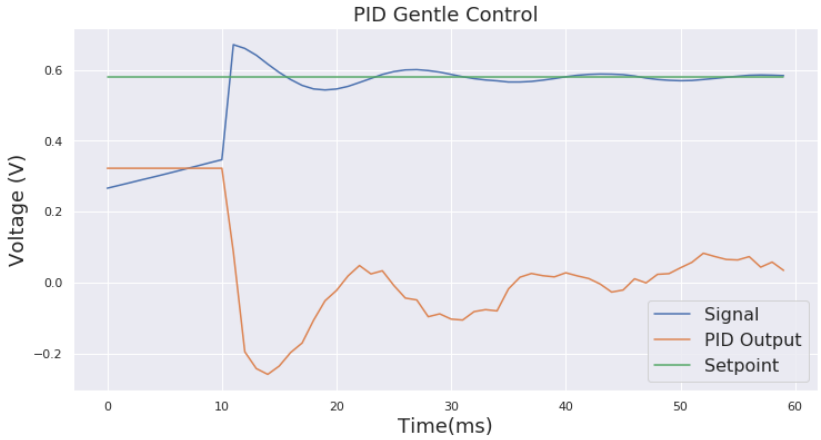

Figure 5: Feedback System with Tuned Parameters. The parameters were set to $K_p = 2, K_i = 4.5, K_d = 2.7$. Notice similar signal behavior but less aggressive control.

3.3 Digital to Analog Conversion

The least interesting, but most difficult component of the entire feedback circuit rests in the actual conversion from a digital number to an analog voltage used to drive the AOM. Our current Digital to Analog Converter (DAC) is an Analog Devices AD5780 mounted to an evaluation board. The evaluation board allows several particular Links, denoted by LK. These links determine several important settings for the AD5780. The ones changed from the default are documented here.

Table 1: LK Settings on AD5780

LK	VSetting
LK1 Position B	Digital Power Supply now J1
LK2 Position A	On board Positive reference $+5V$
LK7 removed	LDAC at logic high
LK8 Position B	On board negative reference AGND
LK11 Removed	DAC accesible at VOUT instead of VOUT Buffered

The current configuration requires two voltage sources. 5V and a ground are supplied to J1, denoted by VCC and DGND. These power the AD5780 IC itself. In addition, voltages anywhere in the range of $\pm(7.5 - 16)$V must be supplied to J2. Positive voltage is between VDD and AGND while negative voltage is between VCC and AGND. These voltages serve as the reference voltages read by the AD5780.
The next configuration requirement is the actual SPI pins. The SPI communication requires 6 different pin connections. The crux of SPI communication is that a tremendous amount of logical information is able to be sent over a single pin through syncing the logical bits to clock cycles. SPI functions through a Master-Slave relationship. The Master Device, here the microcontroller, sets a Slave Select (SS) pin low to determine the other device is a Slave. The AD5780 also requires the LDAC pin to be set low while data is transferred. While these pins are held low, Information is either sent through the Master Out, Slave In (MOSI) pin, or through the Master In, Slave Out, (MISO) pin. These are synced to a CLCK pin. The sixth pin is DGND.

Table 2: SPI Pins

uC32 Pin Number	SPI Connection	Colour
10	SS	Blue
11	MOSI	Red
12	MISO	Orange
13	CLCK	White
9	LDAC	Green
6	DGND	Black

SPI has four modes for how the SPI is configured to the clock cycle. the CPOL bit represents the clock polarity. If this is 0 or 1 means the clock is idle when high or low. Meanwhile the CPHA bit represents clock phase. This represents if the data is shift out on the rising or falling edge. [1] [?] For the AD5780, it requires data sampled on the falling edge and shifted out on the rising edge. This corresponds to CPHA = 1 and CPOL either 0 or 1. These are referred to by AD as SPIMODE 1 or 2 and by Arduino as SPIMODE 1 or 3. In order to establish these parameters, the AD Drivers call a C++ program titled Communication.cpp.

```
SPISettings spiSettings;
unsigned char SPI_Init(unsigned char lsbFirst,
                       unsigned long clockFreq,
                       unsigned char clockPol,
                       unsigned char clockEdg)
{
        int spiMode = 1;
        //decode modes according to https://www.arduino.cc/en/Reference/SPI
        if(clockPol == 0) {
                spiMode = clockEdg ? SPI_MODE1 : SPI_MODE0;
        } else {
                spiMode = clockEdg ? SPI_MODE3 : SPI_MODE2;
        }
        int bitOrder = lsbFirst ? LSBFIRST : MSBFIRST;
        //modify SPI settings object used in transactions
        spiSettings = SPISettings(clockFreq, bitOrder, spiMode);

        //set slave-select pins to output
```

```
        PinMgt_PinOutput(PIN_ID_AD57XX_SLAVE_SELECT);
}
```

This calls the Arduino SPISettings module, which determines all the important settings for SPI communication. The current settings has been changed to CPHA = 0 , CPOL = 1, for SPIMODE1, which is the requested information transfer for the AD5780.
The data itself is sent to four different registers. This is established via the first four bits sent into the AD5780. The first bit R/W is set to 1 for writing to the AD5780. The next three bits establish the address for the register information is being sent to.
An advantage of the AD drivers currently in implementation is that these addresses are established in the header files called, rather than needing to be defined by the user. The current software calls the CTRL register to initialize the AD5780 and then the CLEAR register to establish a zero value voltage for the DAC. Within the loop, the voltage values are then sent to the DAC register to output voltages. The actual output voltage follows the formula

$$V_{OUT} = \frac{(V_{REFP} - V_{REFN}) \times D}{2^{18}} + V_{REFN}$$

where the reference voltages are determined by inputs to J2 and LK2 and LK8 defined above. There is a fourth register, not used, which allows some program-ability in lieu of setting LDAC or SYNC pins. All of these registers take 18 bits of information and discard the last 2. The current drivers store these 24 bits of information in a 4 byte integer. A current unresolved bug lies in the extra byte of empty values seems to be interferring with the order of the data being transferred. the conclusion from PERC is that the chipKIT compiles the the transferred data bytes differently than the Arduino does.

4 Future Work

Once the DAC is up and running, the exciting parts of the digital feedback system would begin.

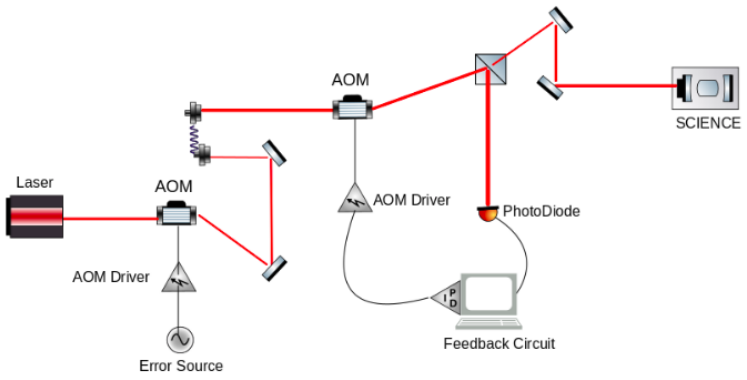

Figure 6: A diagram illustrating the ideal test set up. An additional AOM provides simulated noise which can be corrected via the digital feedback circuit set-up shown on the right hand side.

In order to realize this experimental set-up, the current lab requires development of an working laser diode with temperature and power stabilization. Then would be considerable optical table set-up. The diagram notes two mirrors at positions where fibre coupling is necessary because both position and angle need to be corrected.

Once the experimental set-up is established the PID needs to be tuned. While the Ziegler–Nichols heuristic method mentioned in Section 3.2.1 would be sufficient, the Arduino library has additional potential through the Auto-Tune Library. While this has no documentation or commented code, it has an active Google Groups forum. Autotuned PIDs take information about the peak height and frequency of the correction signal in order to extrapolate the required aggressiveness of the PID control. The library, if realized, also allows for more accurate detection of extrema in the noisy signal, and allows for tunable noise thresholds. All of these combined allow for a more accurate and more stable output signal. This has tremendous advantage if there turn out to be delays in AOM responsitivity time.

5 Conclusion

In conclusion, digital feedback systems remain a powerful tool to improve the performance of laser cooling systems present in the current BEC experiment. Realizing these systems would lead to more accurate data and perhaps more significant scientific results. A particular advantage of digital feedback systems would be the increased bandwidth. These smaller time scales would allow for feedback on laser beams present only for 1ms. Because of this, a particular application of this digital feedback circuit would be for DKC.

References

[1] Arduino spi reference manual.

[2] chipkit uc32 reference manual.

[3] Pic32 reference manual.

[4] Hubert Ammann and Nelson Christensen. Delta kick cooling: A new method for cooling atoms. *Physical Review Letters*, 78(11):2088–2091, 1997.

[5] M H Anderson, Ensher, Matthews, Weiman, and E A Cornel. Observation of bose-einstein condensation in a dilute atomic vapor. *Science*, 269(5221):198–201, Jul 1995.

[6] Bose. Plancks gesetz und lichtquantenhypothese. *Zeitschrift for Physik*, 26(1):178–181, 1924.

[7] Albert Einstein. Quantum theory of a monoatomic ideal gas. *Physikalisch-mathematische Klasse*, 1925.

[8] Harold J. Metcalf and Peter Van der Straten. *Laser cooling and trapping*. Springer, 2002.

[9] Shreyas Potnis. *Tunneling Dynamics of a Bose-Einstein Condensate*. PhD thesis, 2016.

[10] Ramón Ramos, David Spierings, Shreyas Potnis, and Aephraim M. Steinberg. Atom-optics knife edge: Measuring narrow momentum distributions. *Physical Review A*, 98(2), 2018.

[11] Tim Westcott. Pid without a phd. *Embedded Systems Programming*, page 86–108, Oct 2000.